GEOPHYSICS, VOL. 79, NO. 6 (NOVEMBER-DECEMBER 2014); P. KS51–KS60, 6 FIGS.
10.1190/GEO2013-0390.1

Joint location of microseismic events in the presence of velocity uncertainty

Oleg V. Poliannikov[1], Michael Prange[2], Alison E. Malcolm[3], and Hugues Djikpesse[2]

ABSTRACT

The locations of seismic events are used to infer reservoir properties and to guide future production activity, as well as to determine and understand the stress field. Thus, locating seismic events with uncertainty quantification remains an important problem. Using Bayesian analysis, a joint probability density function of all event locations was constructed from prior information about picking errors in kinematic data and explicitly quantified velocity model uncertainty. Simultaneous location of all seismic events captured the absolute event locations and the relative locations of some events with respect to others, along with their associated uncertainties. We found that the influence of an uncertain velocity model on location uncertainty under many realistic scenarios can be significantly reduced by jointly locating events. Many quantities of interest that are estimated from multiple event locations, such as fault sizes and fracture spacing or orientation, can be better estimated in practice using the proposed approach.

INTRODUCTION

Locating seismic events is an important problem in global seismology and in reservoir exploration. Applications of this problem vary in scale from earthquake characterization to hydraulic fracture monitoring. Traditionally, events are located individually, for example, from variants of Geiger's method by ray tracing them from receiver locations using their respective arrival time and polarization estimates. It has been shown (Richards et al., 2006; Hulsey et al., 2009; Eisner et al., 2010; Kummerow, 2010) that this approach ignores important information that couples data from different events and thus ties them together.

Event locations are usually understood in either absolute or relative terms (Slunga et al., 1995). Absolute locations are defined globally with respect to a fixed coordinate system. Relative location is the location of an event relative to other events in the vicinity. Suppose that several microseismic events originate from the same fracture; if we move the fracture by moving all events in it by a constant distance in a specified direction, then the absolute locations of those events will change. However, the relative location of any given event in this fracture with respect to all the rest will remain the same. The primary advantage of relative location over absolute location is that it is often less sensitive to the uncertainties in the velocity model that lie between the cluster of events and the receiver array. Because these velocity uncertainties tend to reposition the cluster as a whole, they have a much smaller impact on the relative locations within the cluster (Waldhauser and Ellsworth, 2000; Zhang and Thurber, 2003). At the same time, the reduction of uncertainty in relative location is not achieved automatically (Michelini and Lomax, 2004), and proper analysis is required for quantifying and comparing absolute and relative location uncertainty (Poliannikov et al., 2011, 2013).

The joint location that we advocate in this paper is a way to recover the absolute and relative positions of all recorded events. Given recorded arrival-time data, we will construct a joint location estimator that is a multidimensional probability distribution of the locations of all recorded events. This probability distribution contains a statistical description of the events, including individual event locations as well as the correlations among these locations. Such correlations are in part due to uncertainty in the velocity model.

In most situations, event location is not the final goal, but a step toward a more complete description of geophysical features such as fractures, faults, pressure fronts, etc. Physical quantities, such as

Manuscript received by the Editor 22 October 2013; revised manuscript received 20 June 2014; published online 24 October 2014.
[1]Massachusetts Institute of Technology, Department of Earth, Atmospheric and Planetary Sciences, Earth Resources Laboratory, Cambridge, Massachusetts, USA. E-mail: poliann@mit.edu.
[2]Schlumberger-Doll Research, Department of Mathematics and Modeling, Cambridge, Massachusetts, USA. E-mail: prange@slb.com; hdjikpesse@slb.com.
[3]Formerly, Massachusetts Institute of Technology, Department of Earth, Atmospheric and Planetary Sciences, Earth Resources Laboratory, Cambridge, Massachusetts, USA; presently Memorial University of Newfoundland, Department of Earth Sciences, St. John's, Newfoundland, Canada. E-mail: amalcolm@mit.edu.

fracture spacing and fault orientation, along with their associated uncertainties, can be inferred from the posterior distribution of the event locations and origin times given recorded data is then obtained by Bayes' rule (Tarantola, 2005; Lomax et al., 2009). Fracture spacing, for example, can be thought of as the average distance among the events in neighboring fractures. Fracture size is related to the distance among events in the same fracture. The joint distribution of all event locations may be used to compute any function of those event locations, for example, the mean fracture spacing and its associated uncertainty.

THEORY

Problem setup

We assume that we have N_s events recorded on an array of N_r receivers and that we have some knowledge of the velocity model V. We denote the seismic event locations $\mathbf{s} = \{\mathbf{s}_1, \ldots, \mathbf{s}_{N_s}\}$, where the $\mathbf{s}_i$ are individual event locations. We assume that the possibly heterogeneous seismic velocity model V is uncertain. We suppose that V belongs to some family of admissible velocity models $\mathcal{V}$. The probability distribution $p(V)$ determines the probability of any given velocity model.

Direct arrivals from all events are recorded at receiver locations $\mathbf{r}_j$, and arrival times $\hat{\mathbf{T}} = \{\hat{T}_{\alpha,i,j}\}$ are estimated. Here, $\alpha \in \{P, S, \ldots\}$ denotes the recorded phase, $i \in \{1, \ldots, N_s\}$ the event index, and $j \in \{1, \ldots, N_r\}$ the receiver index. In addition to estimating direct arrival times, we may also correlate arrivals from events i and i' and estimate correlation lags $\hat{\boldsymbol{\tau}} = \{\hat{\tau}_{\alpha,i,i',j}\}$, which are estimates of the arrival time differences among pairs of events.

We assume that the arrival times and lags so obtained are perturbed by Gaussian noise, i.e.,

$$\hat{T}_{\alpha,i,j} = \mathring{T}_i + T_\alpha(\mathbf{s}_i, \mathbf{r}_j|V) + \mathcal{N}(0, \sigma^2_{\alpha,i,j}) \tag{1}$$

$$\hat{\tau}_{\alpha,i,i',j} = \mathring{T}_{i'} - \mathring{T}_i + \tau_\alpha(\mathbf{s}_i, \mathbf{s}_{i'}, \mathbf{r}_j|V) + \mathcal{N}(0, \zeta^2_{\alpha,i,i',j}), \tag{2}$$

where $\mathring{T}_i$ is the unknown origin time of event i, $T_\alpha(\mathbf{s}_i, \mathbf{r}_j|V)$ is the predicted traveltime for phase α in velocity model V,

$$\tau_\alpha(\mathbf{s}_i, \mathbf{s}_{i'}, \mathbf{r}_j|V) = T_\alpha(\mathbf{s}_{i'}, \mathbf{r}_j|V) - T_\alpha(\mathbf{s}_i, \mathbf{r}_j|V) \tag{3}$$

is the predicted lag among the direct arrivals for phase α from events i and i', and $\mathcal{N}(\cdot,\cdot)$ denotes a Gaussian random variable with given mean and variance.

The problem is to estimate all event locations $\mathbf{s}$ from the observed $\hat{\mathbf{T}}$ and $\hat{\boldsymbol{\tau}}$. We are not concerned here with using additional data that may be available such as the polarization of the incoming waves. Our goal is to better use available kinematic data. When the noise in polarization data can be assumed uncorrelated with that in kinematic data, results from a separate polarization analysis may be combined with those from our proposed methodology by simply multiplying the respective probability density functions.

Joint location in a known velocity model

Before tackling the entire problem of joint location in an uncertain velocity model, we begin with a simplified case in which the velocity model is known. The data likelihood function $p(\hat{\mathbf{T}}, \hat{\boldsymbol{\tau}} \mid \mathbf{s}, \mathring{\mathbf{T}}, V)$ describes the probability of observing $\hat{\mathbf{T}}$ and $\hat{\boldsymbol{\tau}}$, given prescribed event locations $\mathbf{s}$ and origin times $\mathring{\mathbf{T}}$. Under the assumptions stated in the previous section, the likelihood function has the form,

$$p(\hat{\mathbf{T}}, \hat{\boldsymbol{\tau}}|\mathbf{s}, \mathring{\mathbf{T}}, V) \propto \exp\left[-\frac{1}{2}\sum_{\alpha,i,j}\left(\frac{\hat{T}_{\alpha,i,j} - \mathring{T}_i - T_\alpha(\mathbf{s}_i, \mathbf{r}_j|V)}{\sigma_{\alpha,i,j}}\right)^2\right] \times \exp\left[-\frac{1}{2}\sum_{\alpha,i<i',j}\left(\frac{\hat{\tau}_{\alpha,i,i',j} - \tau_\alpha(\mathbf{s}_i, \mathbf{s}_{i'}, \mathbf{r}_j \mid V) - \mathring{T}_{i'} + \mathring{T}_i}{\zeta_{\alpha,i,i',j}}\right)^2\right], \tag{4}$$

in which the normalization constant is dropped for brevity. It is assumed here that the noise in estimated arrival times and lags, and hence $\hat{\mathbf{T}}$ and $\hat{\boldsymbol{\tau}}$, are uncorrelated. When $\hat{\mathbf{T}}$ and $\hat{\boldsymbol{\tau}}$ are correlated separately or jointly, the right side of equation 4 will contain a corresponding covariance matrix that describes this correlation. If only a subset of measurements is available, then the summation is understood to go over the available phases. The posterior distribution of the event locations and origin times in the given data is then obtained by Bayes' rule (Tarantola, 2005; Lomax et al., 2009):

$$\begin{aligned} p(\mathbf{s}, \mathring{\mathbf{T}}|\hat{\mathbf{T}}, \hat{\boldsymbol{\tau}}, V) &= \frac{p(\hat{\mathbf{T}}, \hat{\boldsymbol{\tau}}|\mathbf{s}, \mathring{\mathbf{T}}, V)p(\mathbf{s}, \mathring{\mathbf{T}}|V)}{\iint p(\hat{\mathbf{T}}, \hat{\boldsymbol{\tau}}|\mathbf{s}, \mathring{\mathbf{T}}, V)p(\mathbf{s}, \mathring{\mathbf{T}}|V)\ \mathrm{d}\mathring{\mathbf{T}}\,\mathrm{d}\mathbf{s}} \\ &\propto p(\hat{\mathbf{T}}, \hat{\boldsymbol{\tau}}|\mathbf{s}, \mathring{\mathbf{T}}, V)p(\mathbf{s}, \mathring{\mathbf{T}}|V) \\ &\propto p(\hat{\mathbf{T}}, \hat{\boldsymbol{\tau}} \mid \mathbf{s}, \mathring{\mathbf{T}}, V)p(\mathbf{s}, \mathring{\mathbf{T}}), \end{aligned} \tag{5}$$

in which we assume in the last expression that the prior $p(\mathbf{s}, \mathring{\mathbf{T}})$ is independent of the velocity model.

Throughout the paper, we will assume that the prior distribution of the locations and their origin times is Gaussian; i.e., $p(\mathbf{s}, \mathring{\mathbf{T}}) \sim \mathcal{N}(\boldsymbol{\mu}, \Sigma)$. In numerical simulations, we will use flat priors (infinite variances) to remove the effect of a prior on shown results. The choice of a prior is very important in any Bayesian inversion. We do not address it any further in this work.

If we are interested just in the event locations and not their origin times, then we simply integrate the posterior distribution given in equation 5 over all origin times $\mathring{\mathbf{T}}$ yielding

$$\begin{aligned} p(\mathbf{s}|\hat{\mathbf{T}}, \hat{\boldsymbol{\tau}}, V) &= \int p(\mathbf{s}, \mathring{\mathbf{T}}|\hat{\mathbf{T}}, \hat{\boldsymbol{\tau}}, V)\mathrm{d}\mathring{\mathbf{T}} \\ &\propto \underbrace{\int p(\hat{\mathbf{T}}, \hat{\boldsymbol{\tau}}|\mathbf{s}, \mathring{\mathbf{T}}, V)p(\mathbf{s}, \mathring{\mathbf{T}})\mathrm{d}\mathring{\mathbf{T}}}_{I(\mathbf{s})}. \end{aligned} \tag{6}$$

The integral $I(\mathbf{s})$ in equation 6 can be computed analytically when the integrand is Gaussian with respect to $\mathring{\mathbf{T}}$:

$$\begin{aligned} I(\mathbf{s}) &= \int p(\hat{\mathbf{T}}, \hat{\boldsymbol{\tau}}|\mathbf{s}, \mathring{\mathbf{T}}, V)p(\mathbf{s}, \mathring{\mathbf{T}})\mathrm{d}\mathring{\mathbf{T}} \\ &\propto \int \exp\left[-\frac{1}{2}\mathring{\mathbf{T}}^* A\mathring{\mathbf{T}} + B^*\mathring{\mathbf{T}} + C\right]\mathrm{d}\mathring{\mathbf{T}} \\ &\propto \exp\left[\frac{1}{2}B^*A^{-1}B + C\right], \end{aligned} \tag{7}$$

where A, B, and C are defined in Appendix A.

Gaussian approximation of the joint distribution

Although the posterior joint distribution of event locations can be written exactly, it may be difficult to use in practice. Assuming for simplicity that we are interested in the event locations only, and having marginalized the origin times as spelled out in the previous section, the joint distribution is a function of $3N_s$ variables that needs to be computed numerically. Properly normalizing it requires the evaluation of the right side of equation 6 at all $\mathbf{s}$. Although conceptually straightforward, this computation is numerically costly when N_s becomes large. To simplify the computation and representation of the distribution, we will approximate the posterior distribution with a multivariate normal distribution:

$$p(\mathbf{s}|\hat{\mathbf{T}},\hat{\boldsymbol{\tau}},V)\sim\mathcal{N}(\mathbf{s}^0,\Sigma_{\mathbf{s}}). \tag{8}$$

This approximates the distribution by its first two moments and is appropriate when examining the covariance structure in a joint distribution. If the posterior is well approximated by a multinormal distribution, its mean $\mathbf{s}^0$ and covariance matrix $\Sigma_{\mathbf{s}}$ are found as follows: The mean $\mathbf{s}^0$ is found by solving the maximization problem

$$\mathbf{s}^0=\arg\max_{\mathbf{s}} I(\mathbf{s}), \tag{9}$$

and a local estimate of the covariance about $\mathbf{s}^0$ is given by

$$(\Sigma_{\mathbf{s}}^{-1})_{m,n}\approx-\left.\frac{\partial^2\log I(\mathbf{s})}{\partial s_m\partial s_n}\right|_{\mathbf{s}=\mathbf{s}^0}, \tag{10}$$

where s_m and s_n span all $3N_s$ coordinates of all event locations. If the posterior is not well approximated by a multinormal distribution, the mean and covariance that provide the best fit may be estimated by a sampling approach, such as the Markov chain Monte Carlo.

Joint location in uncertain velocity model

Equations 5 and 8 provide expressions for the posterior distribution given a known velocity model. When the velocity model is uncertain, i.e., it is sampled from a family of admissible velocity models $\mathcal{V}$, we obtain the velocity-independent form of the posterior by conditioning on the velocity V:

$$p(\mathbf{s},\mathring{\mathbf{T}}|\hat{\mathbf{T}},\hat{\boldsymbol{\tau}})\propto\mathsf{E}_V[p(\hat{\mathbf{T}},\hat{\boldsymbol{\tau}}|\mathbf{s},\mathring{\mathbf{T}},V)p(\mathbf{s},\mathring{\mathbf{T}})], \tag{11}$$

where $\mathsf{E}_V[\cdot]$ denotes the expectation over all $V\in\mathcal{V}$. See Appendix B for the derivation of equation 11. If we are interested just in the locations $\mathbf{s}$, then we can, as before, integrate the posterior of $(\mathbf{s},\mathbf{T})$ over $\mathbf{T}$:

$$\begin{aligned}p(\mathbf{s}|\hat{\mathbf{T}},\hat{\boldsymbol{\tau}})&=\int p(\mathbf{s},\mathring{\mathbf{T}}|\hat{\mathbf{T}},\hat{\boldsymbol{\tau}})\,\mathrm{d}\mathring{\mathbf{T}}\\&=\mathsf{E}_V\left[\int p(\hat{\mathbf{T}},\hat{\boldsymbol{\tau}}|\mathbf{s},\mathring{\mathbf{T}},V)p(\mathbf{s},\mathring{\mathbf{T}})\,\mathrm{d}\mathring{\mathbf{T}}\right].\end{aligned} \tag{12}$$

The integral inside the expectation is computed analytically as spelled out in equation 7 and below. To compute the velocity-independent distribution numerically, we generate L velocity models $\{V_l\}_{l=1}^L$ from $\mathcal{V}$, compute the products of the likelihood function and the prior in parallel, and average them. Equations 11 and 12 are general and do not require any assumptions on the specific form of the distributions in the right sides. However, if the distributions inside the expectations are Gaussian, then the resulting posterior in the left side will be a Gaussian mixture.

It may be tempting to estimate the event location uncertainty by averaging velocity-dependent posteriors. For example, we could locate events in several plausible velocity models and use the observed variation as a measure of uncertainty. As explained in Appendix B, this approach to uncertainty quantification is valid when the traveltime data are statistically independent of the velocity; i.e., no additional characterization of the velocity model by tomography using microseismic data is possible. When that assumption is not satisfied, this method may lead to biased location estimates and/or incorrectly estimated uncertainties.

Quantities of interest

Estimated locations of seismic events are often not the final goal of seismic monitoring. The interest is typically in geologic features that the estimated seismic event locations can help to reveal (Michaud et al., 2004; Bennett et al., 2005; Huang et al., 2006). Assuming that most microseismic events originate in fractures, clouds of microseismic events reveal the fracture size, position, orientation, etc. Such quantities of interest can be written as functionals of the estimated event locations $f(\mathbf{s})$. Because $\mathbf{s}$ is a random vector, $f(\mathbf{s})$ becomes a random variable. We can use probability theory to compute the distribution of $f(\mathbf{s})$ or estimate its statistics.

The mean and variance statistics can be written analytically; e.g.,

$$\mathsf{E}f(\mathbf{s})=\int f(\mathbf{s})p(\mathbf{s}|\hat{\mathbf{T}},\hat{\boldsymbol{\tau}})\mathrm{d}\mathbf{s} \tag{13}$$

or

$$\mathrm{Var}f(\mathbf{s})=\int(f(\mathbf{s})-\mathsf{E}f(\mathbf{s}))^2p(\mathbf{s}|\hat{\mathbf{T}},\hat{\boldsymbol{\tau}})\mathrm{d}\mathbf{s}. \tag{14}$$

Alternatively, the distribution of $f(\mathbf{s})$ can be computed numerically by sampling the joint locations and applying the function f.

NUMERICAL RESULTS

We illustrate the proposed methodology with numerical examples for a typical problem of monitoring with a single borehole array of receivers. We have an isotropic layered velocity model and two fractures, as shown in Figure 1. The 16 receivers are equally spaced in a vertical well at depths from 1700 to 2200 m. Two sets of events from two neighboring fractures, F_1 and F_2 (nine events in each fracture), are situated about 700 and 1000 m away from the monitoring well, respectively. Note that the true event locations have a somewhat irregular geometry; i.e., they are not perfectly coplanar. For illustration purposes, we assume that the velocity in each layer is known approximately up to the same multiplicative factor that is uniformly distributed between -5% and 5%.

We assume that direct arrival times from all events are picked with errors that are normal with zero mean and standard deviation 1 ms. We do not use correlation lag times in this example to demonstrate that joint location, even when acting only on time picks, greatly reduces the impact of velocity uncertainty on event locations. Note that

traveltimes in this setup are completely insensitive to the azimuth of the event locations. We therefore only attempt to reconstruct the distance from the receiver array to the event locations and the event depths.

Event locations

Figure 2a shows the receivers placed at depths from 1700 to 2200 m. The blue ellipses are 95% confidence regions for individual events; they are constructed from the computed posterior densities of individual event locations. The shape and size of the ellipse is controlled by signal noise, aperture geometry, as well as velocity uncertainty. These ellipses, however, do not capture the statistical dependence among the locations of different events induced by the velocity uncertainty.

Event location uncertainty obtained by jointly locating events is hard to directly visualize because it involves a multidimensional correlation matrix. It is still possible to see the manifestation of this uncertainty if we compute the distributions of functions of event locations, e.g., fracture height or fracture spacing.

Estimating fracture characteristics

Let us first pick events that came from the same fracture F_1 and view the difference between the maximal and minimal depths of the events as a simple proxy for the fracture height. Given the joint distribution of the event locations, we can compute the distribution of the fracture height. Toward that end, we generate a sample from the joint distribution and compute the difference between the maximal depth and the minimal depth of the events from the same fracture; i.e.,

$$h(F_1) = \max_{\mathbf{s}\in F_1} s_z - \min_{\mathbf{s}\in F_1} s_z. \tag{15}$$

Figure 2b shows in blue the resulting distribution of the fracture height calculated using the proposed joint location method. We then emulate the conventional individual event location by computing, from the joint distribution, the marginal distributions for individual events. From these distributions, we individually sample each event and compute the fracture height as spelled out in equation 15. The resulting histogram of fracture height calculated from the individually located events is displayed in Figure 2b in red. We can see that by jointly locating microseismic events, we estimate the fracture height much more precisely because the effect of the velocity uncertainty is significantly reduced by properly accounting for the resulting correlation among different events. We illustrate this effect by providing a simple quantitative measure e, which is the ratio of the standard deviation computed from the individual location and that computed from joint location.

We note, as a word of caution, that joint event location does not always lead to smaller uncertainty in the quantity of interest. What joint location does here is mitigate errors in the estimated uncertainty, which come about in conventional individual location when different event locations share the same source of uncertainty.

Consider now pairs of events, one from each fracture, $\mathbf{s}_1 \in F_1$, $\mathbf{s}_2 \in F_2$. The minimal distance among such two events can be viewed as a simple proxy for the fracture spacing:

$$\ell(F_1, F_2) = \min_{\mathbf{s}_1\in F_1, \mathbf{s}_2\in F_2} \|\mathbf{s}_1 - \mathbf{s}_2\|. \tag{16}$$

We compare the minimal distance between the two events from the two fractures, computed from the joint distribution, and the distance estimated just from the marginal distributions of the individual event locations. The resulting histograms for the joint and individual event location are shown in Figure 2c. Joint event location again produces a better estimate of the fracture spacing than individual location does, by correctly handling the correlation among different events induced by velocity uncertainty along shared paths.

Effect of aperture position

Correlation among event locations induced by velocity uncertainty in the model depends on several factors, array location and geometry being among the most important. Figure 3a shows an experiment identical to the one considered previously, but with the receiver array shifted up by 400 m. We see that when the array is above the events, the resulting ray geometry ensures that velocity uncertainty primarily affects reconstructed depths of the events. Consequently, we expect to see the effect of joint event location to be manifested primarily in estimating quantities that depend on event depths. Figure 3b shows a big improvement in estimating the fracture height. The correlation among the horizontal coordinates of the event locations induced by the velocity uncertainty in this geometry is not so significant, so the improvement in estimating fracture spacing from using joint event location is modest as shown in Figure 3c.

When the array is lowered to encompass the depth of the events, as shown in Figure 4a, velocity uncertainty affects the horizontal coordinates of the events more than their depths. Consequently, joint event location improves the estimate of the fracture spacing (Figure 4c), and it has little effect on the estimate of the fracture height (Figure 4b).

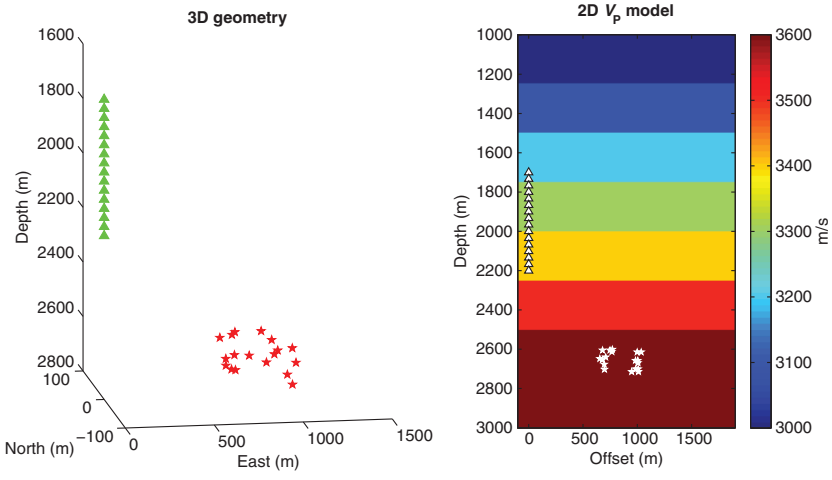

Figure 1. A numerical setup with seven layers, two fractures (each represented by a separate set of events), and 16 borehole receivers located at depths from 1700 to 2200 m. (a) The full 3D setup and (b) the same setup is shown in 2D offset from well-depth domain.

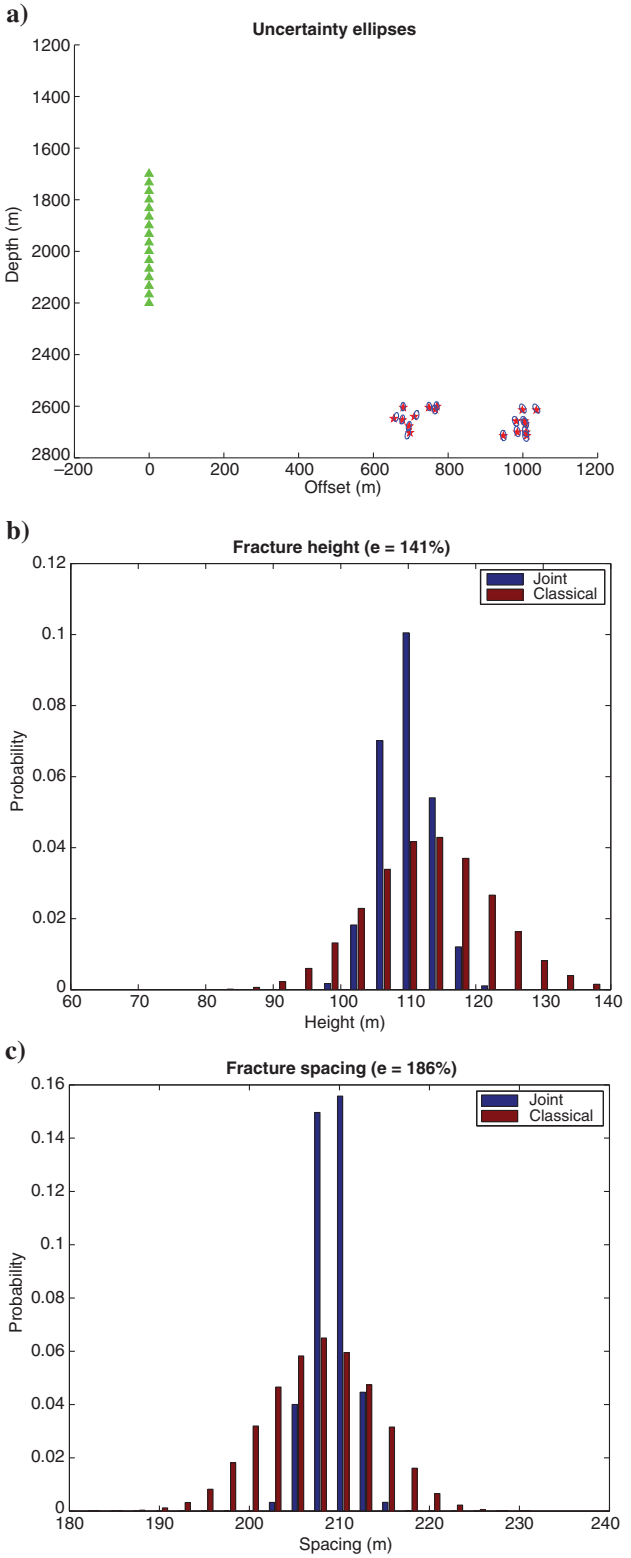

Figure 2. (a) Blue ellipses show 95% confidence regions for individual events. The histogram of estimated fracture spacing, $\ell(F_1, F_2) =$ 210 m; (b) fracture height, $h(F_1) = 110$ m; and (c) using the joint and individual location. The ratio of the standard deviation computed from individual location and that computed from joint location e is provided. The velocity uncertainty is 5%, and time picks are Gaussian with standard deviation of 1 ms.

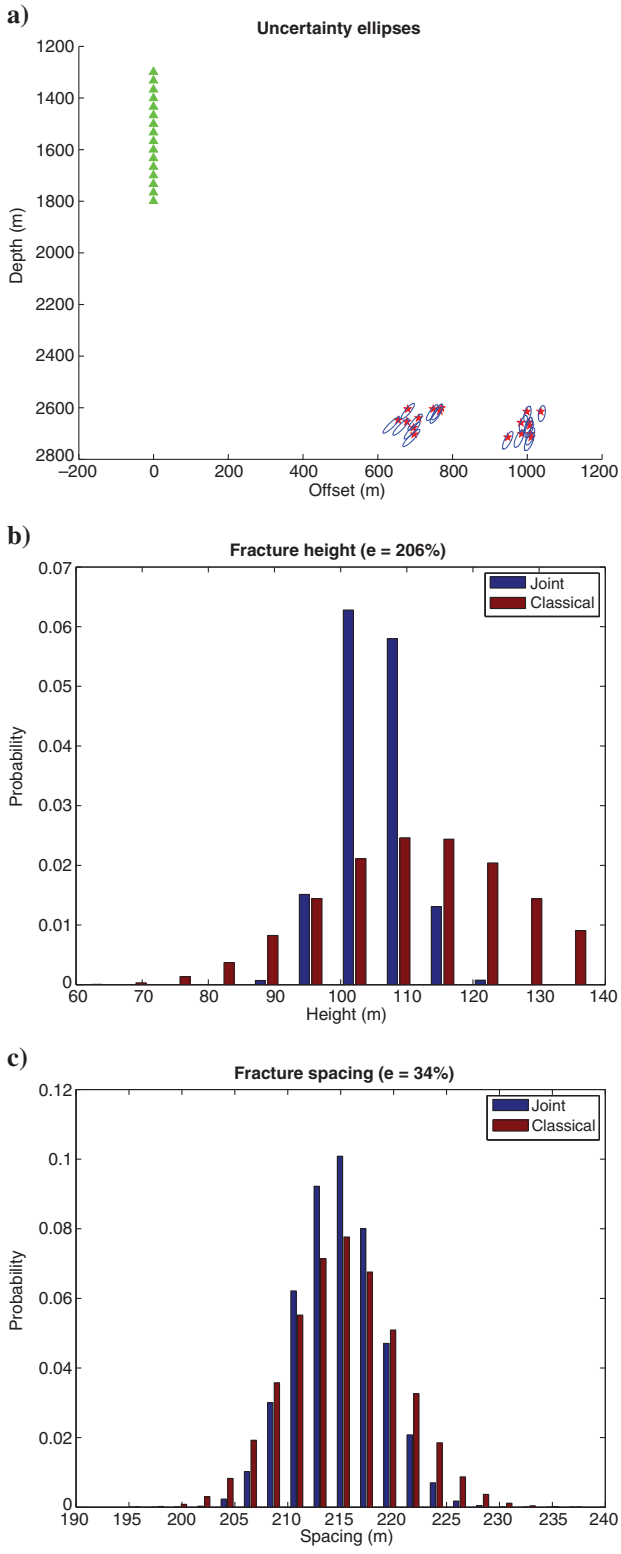

Figure 3. A repeat of the experiment of Figure 2, but with the receiver array shifted up by 400 m.

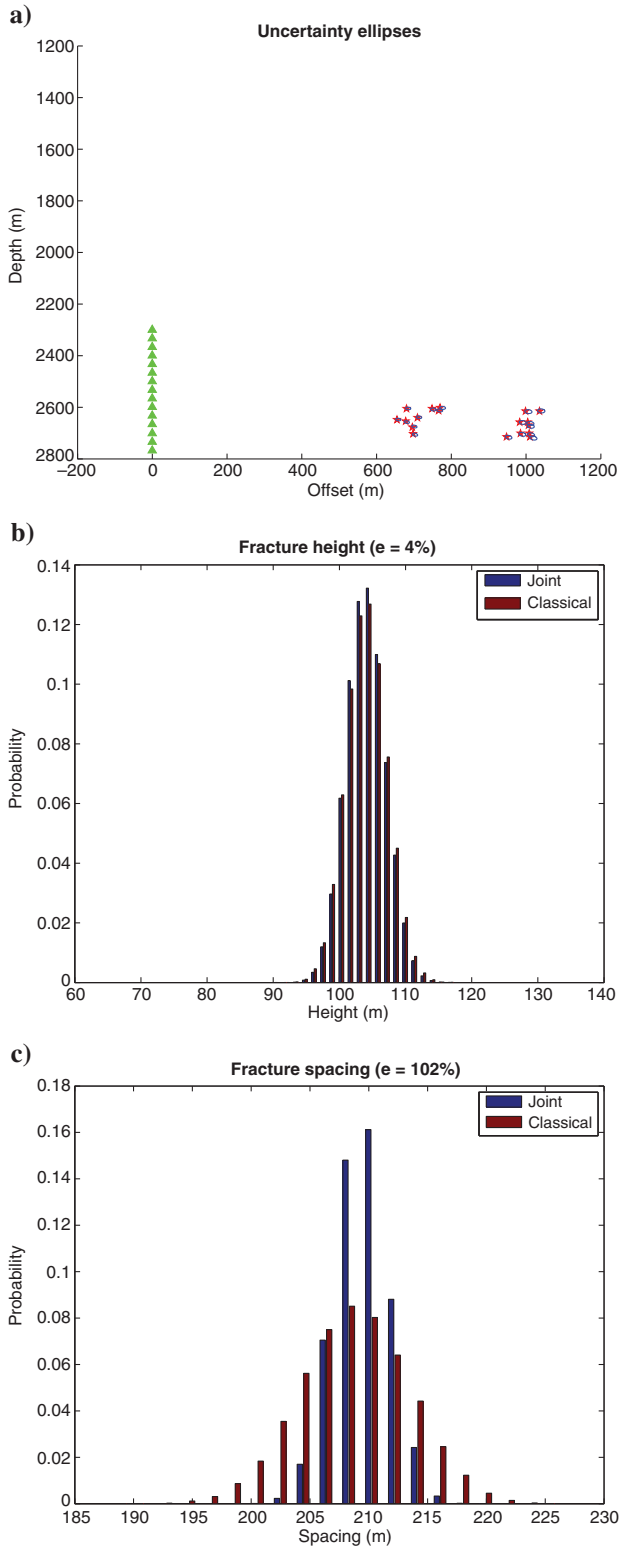

Figure 4. A repeat of the experiment of Figure 2, but with the receiver array shifted down by 600 m.

Velocity uncertainty versus signal noise

We have shown in the examples above that joint event location is superior to individual location because it correctly accounts for the correlation among event locations induced by velocity uncertainty. Joint event location is particularly effective for mitigating the impact of velocity uncertainty on event-location error in the direction of the wave energy connecting two events. This effect is illustrated in the numerical experiment described in Figure 5. Individual location inherently ignores the correlation among event locations and overestimates location uncertainty when velocity uncertainty is the dominant cause of randomness in the problem. When the dominant factor is uncorrelated signal noise, the correlation among different event locations is weak, and the difference between joint and individual location is less prominent.

We illustrate these statements with a series of numerical experiments. Two events are placed in a homogeneous medium, and a vertical array of receivers is positioned nearby as shown in Figure 5. We jointly locate the two events for different levels of velocity uncertainty and different signal noise. Results are shown in Figure 6. Velocity uncertainty increases from top to bottom, and signal noise increases from left to right.

The two extreme cases are shown in the bottom left, in which the velocity uncertainty is the largest but the signal noise is relatively small, and the top right, in which the velocity uncertainty is the smallest but the signal noise is large. Other panels show intermediate cases. We display the distribution of the distance among the two event locations; this distance may serve as a proxy for a fracture spacing estimated from a borehole array or as a proxy for fracture height estimated from a surface array (after rotating the model 90° clockwise).

When the velocity uncertainty is the dominant factor (bottom left), joint event location leads to much smaller uncertainty in the estimate of the distance among the two events. When the signal noise is dominant (top right), the difference among the results of joint and individual location is less pronounced. This illustrates that estimates obtained from joint location are superior to estimates

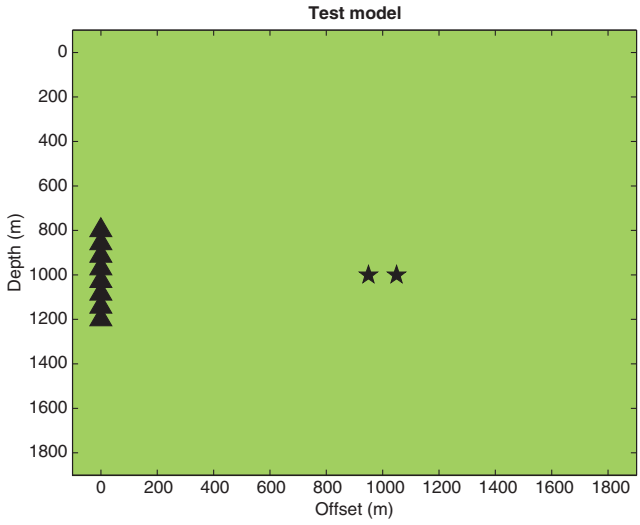

Figure 5. A homogeneous test model with two events and eight receivers nearby.

obtained from individual location when velocity uncertainty is dominant over signal noise. Independence of event locations, implicitly assumed by individual location, ignores information about the correlation among event locations induced by velocity uncertainty, and hence leads to larger uncertainties in the location estimates.

SUMMARY WORKFLOW

In this section, we summarize our method and highlight important differences between our method and other techniques with the help of a workflow. We assume that microseismic data are collected in the field. The goal is to characterize locations of all recorded events.

Prior distribution

A prior distribution of the events represents our knowledge of the event locations before microseismic data have been processed. It may be informed by well geometry, location of perforation shots, etc. If some event locations are assumed known (master events) $\mathbf{s} = \mathbf{s}_0$, then the prior will contain delta functions $\delta(\mathbf{s} - \mathbf{s}_0)$. An uninformed prior can be obtained by taking a Gaussian distribution with very large variances. An informative/restrictive prior will have considerable effect on location results. The proposed methodology cannot validate priors, but their effect on the reconstructed locations can be studied by varying them.

Velocity model

We describe a velocity model by a numerical sampler from a probability distribution $p(V)$. An example $p(V)$ might be a distribution of values of velocity for a particular layer. If the velocity model $V = V_0$ is assumed known, then $p(V) = \delta(V - V_0)$. It is common in literature to assume that the velocity model is known. As with the location priors, location analysis cannot validate or rule out velocity priors unless they lead to obviously unphysical results. It is usually understood that the assumed velocity model contains uncertainty. We argue that when tomography is performed, this uncertainty should be quantified and used as input in subsequent analysis. It is possible in principle to invert for microseismic event locations and the velocity model simultaneously, but the resulting locations and velocity model are bound to have uncertainties and trade-offs that should be quantified by a joint distribution.

Arrival times and lags

The recorded data are processed, and P and/or S arrival times of each event are estimated along with their uncertainties. There is no requirement to detect P and S arrival for each recorded event. However, it is required that the recorded phases can be modeled using the available velocity model. For example, if body waves are recorded, then body waves (and not head waves) should be modeled. We can also estimate time lags, such as S − P, or lags among similar phases of different events as used in double-difference or interferometry, by either subtracting traveltimes or crosscorrelating waveforms. Care must be taken to avoid double counting data. For example, if P and S arrivals are included in the data, then S − P cannot be included. Formally, this issue is resolved by including an assumed correlation structure of the data into the likelihood function. Beyond using this correlation matrix, there is no weighing of data prior to calculating the posterior distribution of event locations.

Calculating the posterior

The likelihood function is given by equation 4 or 7, and it along with the prior can be computed for any set of event locations and any velocity model. The Gaussian approximation to the posterior distribution of the event location is calculated using equations 9 and 10 (or by using a sampler if the Gaussian approximation is inappropriate). The application to just a single event would reduce our method to conventional individual location.

Computing fracture properties

Some fracture properties, such as height, spacing, etc, can be approximated as functions of event locations. There is no predefined function for each quantity of interest, and the user is free to design any appropriate function. The distribution of such a quantity, including its mean and standard deviation, can be computed from the joint distribution.

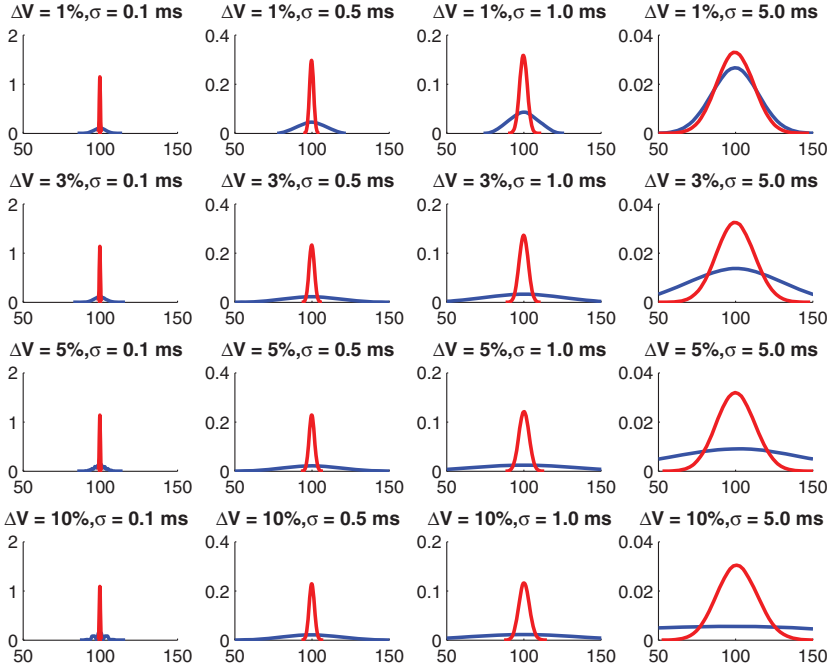

Figure 6. A comparison of the distributions of the distance among the two events shown in Figure 5 obtained using the individual (blue) and joint (red) location. Each panel corresponds to a different choice of velocity uncertainty and signal noise. The horizontal axis is the fracture distance, and the vertical axis is the probability density function (PDF) value. A wider curve means more uncertainty.

CONCLUSIONS

In this paper, we have proposed a new method for simultaneously locating multiple seismic events in the presence of an uncertain velocity model. This method includes absolute as well as relative event locations, without requiring that any reference or master events be known. The method uses any available kinematic data, such as P or S traveltimes or correlation lags, without artificial constraints such as the availability of P and S arrivals for the same event.

Event locations always carry uncertainty induced by several factors such as signal noise, location and geometry of the array aperture, and, most importantly in many applications, uncertainty in the velocity model. Velocity uncertainty induces correlation in traveltimes from the event location to the receiver array, and hence in event locations. Joint location captures this correlation by simultaneously registering all event locations in each sampled velocity model.

In many applications, the model geometry is such that raypaths from events to receivers largely overlap, allowing the possibility of shared-path cancellation. In this case, the effect of the velocity uncertainty along shared paths is mitigated resulting in better relative location. The proposed approach captures positive aspects of double-difference and interferometry that also use this effect, without requiring the differencing of traveltimes.

Joint location does not guarantee smaller uncertainty. It provides a more accurate estimator of event locations and their associated uncertainty by capturing the entire covariance structure over all the events. We visualize the effect of joint location uncertainty through its impact on functionals of event locations, such as fracture height or spacing. This impact can be visualized with simple 1D histograms.

ACKNOWLEDGMENTS

We thank W. Rodi of MIT for extremely useful discussions. We acknowledge the funding provided by the ERL Founding Members Consortium and National Science Foundation under grant no. SES-0962484.

APPENDIX A

INTEGRATING OVER ORIGIN TIMES

The matrix A, vector B, and scalar C in equation 7 are defined as follows:

$$\mathbf{A} = \mathbf{A^L} + \mathbf{A^P}, \quad \mathbf{B} = \mathbf{B^L} + \mathbf{B^P}, \quad \text{and } C = C^{\mathrm{L}} + C^{\mathrm{P}},$$

in which the right sides are contributions of the likelihood function and prior. The expressions for the contributions from the likelihood function are as follows:

$$A^{\mathrm{L}}_{i,i'} = \sum_{\alpha,j} \frac{1}{\sigma^2_{\alpha,i,j}} + \sum_{\alpha,i''<i,j} \frac{1}{\zeta^2_{\alpha,i'',i,j}} + \sum_{\alpha,i<i'',j} \frac{1}{\zeta^2_{\alpha,i'',i,j}}, \quad i = i'';$$

$$A^{\mathrm{L}}_{i,i'} = -2\sum_{\alpha,j} \frac{1}{\zeta^2_{\alpha,i,i'',j}}, \quad i < i'';$$

$$A^{\mathrm{L}}_{i,i'} = 0, \quad i > i'', \tag{A-1}$$

$$B^{\mathrm{L}}_i = \sum_{\alpha,j} \frac{\hat{T}_{\alpha,i,j} - T_\alpha(\mathbf{s}_i, \mathbf{r}_j|V)}{\sigma^2_{\alpha,i,j}} + \sum_{\alpha,i'<i,j} \frac{\hat{\tau}_{\alpha,i',i,j} - \tau_\alpha(\mathbf{s}_{i'}, \mathbf{s}_i, \mathbf{r}_j|V)}{\zeta^2_{\alpha,i',i,j}} - \sum_{\alpha,i<i',j} \frac{\hat{\tau}_{\alpha,i,i',j} - \tau_\alpha(\mathbf{s}_i, \mathbf{s}_{i'}, \mathbf{r}_j|V)}{\zeta^2_{\alpha,i,i',j}}, \tag{A-2}$$

$$C^{\mathrm{L}} = -\frac{1}{2}\sum_{\alpha,i,j} \frac{(\hat{T}_{\alpha,i,j} - T_\alpha(\mathbf{s}_i, \mathbf{r}_j|V))^2}{\sigma^2_{\alpha,i,j}} - \sum_{\alpha,i<i',j} \frac{(\hat{\tau}_{\alpha,i,i',j} - \tau_\alpha(\mathbf{s}_i, \mathbf{s}_{i'}, \mathbf{r}_j|V))^2}{\zeta^2_{\alpha,i,i',j}}. \tag{A-3}$$

The contributions from the priors are written as

$$\begin{aligned}
\mathbf{A^P} &= M_{22}, \\
\mathbf{B^P} &= -\frac{1}{2}[(\mathbf{s} - \boldsymbol{\mu}_{\mathbf{s}})^*(M_{12} + M^*_{21}) - \boldsymbol{\mu}^*_{\mathring{\mathbf{T}}}(M_{22} + M^*_{22})], \\
C^{\mathrm{P}} &= -\frac{1}{2}[(\mathbf{s} - \boldsymbol{\mu}_{\mathbf{s}})^* M_{11}(\mathbf{s} - \boldsymbol{\mu}_{\mathbf{s}}) - \boldsymbol{\mu}^*_{\mathring{\mathbf{T}}} M_{21}(\mathbf{s} - \boldsymbol{\mu}_{\mathbf{s}}) \\
&\quad - (\mathbf{s} - \boldsymbol{\mu}_{\mathbf{s}}) M_{12}\boldsymbol{\mu}_{\mathring{\mathbf{T}}} + \boldsymbol{\mu}^*_{\mathring{\mathbf{T}}} M_{22}\boldsymbol{\mu}_{\mathring{\mathbf{T}}}],
\end{aligned} \tag{A-4}$$

where we put by definition

$$\boldsymbol{\mu} = \begin{pmatrix} \boldsymbol{\mu}_{\mathbf{s}} \\ \boldsymbol{\mu}_{\mathring{\mathbf{T}}} \end{pmatrix} \text{ and } \Sigma^{-1} = \begin{pmatrix} M_{11} & M_{12} \\ M_{21} & M_{22} \end{pmatrix}.$$

APPENDIX B

VELOCITY MARGINALIZATION

In this section, we derive the exact formula for a velocity-independent posterior distribution of the event location and discuss a natural and often useful approximation to the exact solution. We use the symbols $\hat{\mathbf{T}}$, V, $\mathbf{s}$, and $\mathring{\mathbf{T}}$ to refer to the traveltime data, the velocity model, the event locations, and the event origin times. Assume we have a proper likelihood function $p(\hat{\mathbf{T}}|\mathbf{s}, \mathring{\mathbf{T}}, V)$ and priors on the velocity and event location $p(V)$ and $p(\mathbf{s})$. The velocity prior does not include information from $\hat{\mathbf{T}}$. The posterior on $\mathbf{s}$ and V is then given by

$$p(\mathbf{s}, \mathring{\mathbf{T}}, V|\hat{\mathbf{T}}) = \frac{p(\hat{\mathbf{T}}|\mathbf{s}, \mathring{\mathbf{T}}, V)p(\mathbf{s}, \mathring{\mathbf{T}})p(V)}{p(\hat{\mathbf{T}})}, \tag{B-1}$$

where

$$p(\hat{\mathbf{T}}) = \iiint p(\hat{\mathbf{T}}|\mathbf{s}, \mathring{\mathbf{T}}, V)p(\mathbf{s}, \mathring{\mathbf{T}})p(V)\,\mathrm{d}\mathbf{s}\,\mathrm{d}\mathring{\mathbf{T}}\,\mathrm{d}V. \quad \text{(B-2)}$$

Information on $\mathbf{s}$ and $\mathring{\mathbf{T}}$ can be found from the joint $(\mathbf{s}, \mathring{\mathbf{T}}, V)$-posterior through marginalization:

$$\begin{aligned} p(\mathbf{s}, \mathring{\mathbf{T}}|\hat{\mathbf{T}}) &= \int p(\mathbf{s}, \mathring{\mathbf{T}}, V|\hat{\mathbf{T}})\mathrm{d}V \\ &= \int \frac{p(\hat{\mathbf{T}}|\mathbf{s}, \mathring{\mathbf{T}}, V)p(\mathbf{s}, \mathring{\mathbf{T}})p(V)}{p(\hat{\mathbf{T}})}\mathrm{d}V \\ &= \mathsf{E}_V\left[\frac{p(\hat{\mathbf{T}}|\mathbf{s}, \mathring{\mathbf{T}}, V)p(\mathbf{s}, \mathring{\mathbf{T}})}{p(\hat{\mathbf{T}})}\right] \\ &= \frac{1}{p(\hat{\mathbf{T}})}\mathsf{E}_V[p(\hat{\mathbf{T}}|\mathbf{s}, \mathring{\mathbf{T}}, V)p(\mathbf{s}, \mathring{\mathbf{T}})]. \end{aligned} \quad \text{(B-3)}$$

Information on $\mathbf{s}$ without the origin times $\mathring{\mathbf{T}}$ is then found through an additional integration:

$$p(\mathbf{s}|\hat{\mathbf{T}}) = \frac{1}{p(\hat{\mathbf{T}})}\mathsf{E}_V\left[\int p(\hat{\mathbf{T}}|\mathbf{s}, \mathring{\mathbf{T}}, V)p(\mathbf{s}, \mathring{\mathbf{T}})\,\mathrm{d}\mathring{\mathbf{T}}\right], \quad \text{(B-4)}$$

in which the integral inside the expectation is evaluated just like in equation 7.

The following algorithm of computing the posterior distribution of the event locations directly follows from equation B-3:

1) Given observed traveltime data $\hat{\mathbf{T}}$ for each randomly sampled velocity model V, compute the likelihood function $p(\hat{\mathbf{T}}|\mathbf{s}, \mathring{\mathbf{T}}, V)$.
2) Multiply the likelihood function by the initial prior $p(\mathbf{s}, \mathbf{T})$.
3) Repeat steps 1–2 for other velocity model samples $V \in \mathcal{V}$ and sum the PDF products, until the convergence of the sum is detected. This can be computationally expensive if the family of admissible velocities $\mathcal{V}$ is very large.
4) Normalize this sum so that it integrates to one over $\mathbf{s}$ and $\mathring{\mathbf{T}}$, thus effectively dividing by $p(\hat{\mathbf{T}})$.

Normalizing the posterior by $p(\hat{\mathbf{T}})$ is impractical for a large number of events. However, we can form the unnormalized joint posterior using such methods as Monte Carlo Markov Chains, and hence can compute statistics of this distribution of any function of it.

Averaging velocity-dependent posteriors

Assume in addition to what is stated above that the observed data $\hat{\mathbf{T}}$ is statistically independent of the velocity model V; i.e.,

$$p(\hat{\mathbf{T}}|V) = p(\hat{\mathbf{T}}) \quad \text{or equivalently} \quad p(V|\hat{\mathbf{T}}) = p(V). \quad \text{(B-5)}$$

Note that all probabilities in equation B-5 are integrated over all possible event locations $\mathbf{s}$.

The assumption in equation B-5 means that no velocity model can be deemed more or less likely based on the observed traveltimes alone, without any knowledge of the event. It holds, for example, in a 1D case due to a trade-off between the event location and the velocity. In more practical terms, it is assumed that no additional characterization of the velocity model by tomography using microseismic data is possible. This may be the case when the velocity model was estimated using multiple perforation shots with known locations and high signal-to-noise ratios. Induced microseismicity then may not provide enough additional illumination of the model to allow a better estimate of the velocity.

From equation A-4, we obtain

$$\begin{aligned} p(\mathbf{s}, \mathring{\mathbf{T}}|\hat{\mathbf{T}}) &= \mathsf{E}_V\left[\frac{p(\hat{\mathbf{T}}|\mathbf{s}, \mathring{\mathbf{T}}, V)p(\mathbf{s}, \mathring{\mathbf{T}})}{p(\hat{\mathbf{T}})}\right] \\ &= \mathsf{E}_V\left[\frac{p(\hat{\mathbf{T}}|\mathbf{s}, \mathring{\mathbf{T}}, V)p(\mathbf{s}, \mathring{\mathbf{T}})}{p(\hat{\mathbf{T}}|V)}\right] \\ &= \mathsf{E}_V\left[\frac{p(\hat{\mathbf{T}}, \mathbf{s}, \mathring{\mathbf{T}}, V)p(\mathbf{s}, \mathring{\mathbf{T}})p(V)}{p(\mathbf{s}, \mathring{\mathbf{T}}, V)p(\hat{\mathbf{T}}, V)}\right] \\ &= \mathsf{E}_V\left[\frac{p(\hat{\mathbf{T}}, \mathbf{s}, \mathring{\mathbf{T}}, V)}{p(\hat{\mathbf{T}}, V)}\right] \\ &= \mathsf{E}_V[p(\mathbf{s}, \mathring{\mathbf{T}}|\hat{\mathbf{T}}, V)]. \end{aligned} \quad \text{(B-6)}$$

We have shown that if the condition in equation B-5 is satisfied, then the unconditional posterior distribution of $p(\mathbf{s}, \mathring{\mathbf{T}}|\hat{\mathbf{T}})$ can be obtained by simply averaging velocity-dependent posteriors $p(\mathbf{s}, \mathring{\mathbf{T}}|\hat{\mathbf{T}}, V)$ over different velocity models V. Estimating uncertainty in this way is quite common; however, it is only an approximation to the true uncertainty that gains nothing in computational speed. It should therefore be summarily avoided.

REFERENCES

Bennett, L., J. L. Calvez, D. R. R. Sarver, K. Tanner, W. S. Birk, G. Waters, J. Drew, G. Michaud, P. Primiero, L. Eisner, R. Jones, D. Leslie, M. J. Williams, J. Govenlock, R. C. R. Klem, and K. Tezuka, 2005, The source for hydraulic fracture characterization: Oilfield Review, **17**, 42–57.

Eisner, L., B. J. Hulsey, P. Duncan, D. Jurick, H. Werner, and W. Keller, 2010, Comparison of surface and borehole locations of induced seismicity: Geophysical Prospecting, **58**, 809–820, doi: 10.1111/j.1365-2478.2010.00867.x.

Huang, Y. A., J. Chen, and J. Benesty, eds., 2006, Time delay estimation and acoustic source localization, *in* Acoustic MIMO signal processing: Springer, Signals and Communication Technology, 215–259.

Hulsey, B. J., L. Eisner, M. Thornton, and D. Jurick, 2009, Application of relative location technique from surface arrays to microseismicity induced by shale fracturing: 79th Annual International Meeting, SEG, Expanded Abstracts, 1602–1606.

Kummerow, J., 2010, Using the value of the crosscorrelation coefficient to locate microseismic events: Geophysics, **75**, no. 4, MA47–MA52, doi: 10.1190/1.3463713.

Lomax, A., A. Michelini, and A. Curtis, 2009, Earthquake location, direct, global-search methods, *in* A. Lomax, eds., Encyclopedia of complexity and systems science: Springer, 2449–2473.

Michaud, G., D. Leslie, J. Drew, T. Endo, and K. Tezuka, 2004, Microseismic event localization and characterization in a limited aperture HFM experiment: 74th Annual International Meeting, SEG, Expanded Abstracts, 552–555.

Michelini, A., and A. Lomax, 2004, The effect of velocity structure errors on double-difference earthquake location: Geophysical Research Letters, **31**, L09602, doi: 10.1029/2004GL019682.

Poliannikov, O. V., A. E. Malcolm, H. Djikpesse, and M. Prange, 2011, Interferometric hydrofracture microseism localization using neighboring fracture: Geophysics, **76**, no. 6, WC27–WC36, doi: 10.1190/geo2010-0325.1.

Poliannikov, O. V., M. Prange, A. E. Malcolm, and H. Djikpesse, 2013, A unified Bayesian framework for relative microseismic location: Geophysical Journal International, **194**, 557–571, doi: 10.1093/gji/ggt119.

Richards, P. G., F. Waldhauser, D. Schaff, and W.-Y. Kim, 2006, The applicability of modern methods of earthquake location: Pure and Applied Geophysics, **163**, 351–372, doi: 10.1007/s00024-005-0019-5.

Slunga, R., S. T. Rognvaldsson, and R. Bodvarsson, 1995, Absolute and relative locations of similar events with application to microearthquakes in southern Iceland: Geophysical Journal International, **123**, 409–419, doi: 10.1111/j.1365-246X.1995.tb06862.x.

Tarantola, A., 2005, Inverse problem theory and methods for model parameter estimation: SIAM.

Waldhauser, F., and W. L. Ellsworth, 2000, A double-difference earthquake location algorithm: Method and application to the Northern Hayward Fault, California: Bulletin of the Seismological Society of America, **90**, 1353–1368, doi: 10.1785/0120000006.

Zhang, H., and C. H. Thurber, 2003, Double-difference tomography: The method and its application to the Hayward Fault, California: Bulletin of the Seismological Society of America, **93**, 1875–1889, doi: 10.1785/0120020190.